Imaging of Large Airways Disorders

Benedikt H. Heidinger[1]
Mariaelena Occhipinti
Ronald L. Eisenberg
Alexander A. Bankier

OBJECTIVE. Recent technical advances, including the routine use of CT thin sections and techniques such as 2D minimum-intensity-projection and 3D volume images, have increased our ability to detect large airways diseases. Furthermore, dedicated CT protocols allow the evaluation of dynamic airway dysfunction.

CONCLUSION. With diseases of the large airways more commonly seen in daily practice, it is important that radiologists be familiar with the appearances, differential diagnosis, and clinical implications of these entities.

American Journal of Roentgenology 2015.205:41-56.

Keywords: chest radiography, CT, large airways disorders, tracheobronchomalacia

DOI:10.2214/AJR.14.13857

Received September 9, 2014; accepted after revision December 5, 2014.

A. A. Bankier is a consultant for Spiration (Olympus Medical Systems) and has received authorship honoraria from Elsevier.

[1]All authors: Department of Radiology, Beth Israel Deaconess Medical Center, Harvard Medical School, 330 Brookline Ave, Boston, MA 02215. Address correspondence to R. L. Eisenberg (rleisenb@bidmc.harvard.edu).

This article is available for credit.

AJR 2015; 205:41–56

0361–803X/15/2051–41

The trachea and the main, lobar, and segmental bronchi—down to a diameter of 2–3 mm—are considered to be the "large airways" [1–4], and a wide spectrum of diseases can occur in this anatomic region (Appendix 1). Our ability to identify lesions in this area has been substantially improved by recent advances such as the routine use of volumetric MDCT with thin-section reconstructions and techniques such as 2D minimum-intensity-projection and 3D volume images [1, 5]. Furthermore, dedicated CT protocols allow the evaluation of dynamic airway dysfunction [1, 5]. Dedicated scanning protocols include end-inspiratory CT paired with either dynamic expiratory CT during forceful exhalation or static end-expiratory CT. Cine CT during coughing is also performed for dynamic assessment of the large airways [6, 7]. Imaging of the large airways is indicated if pulmonary function test results show a discrepancy with the clinical presentation—for example, pulmonary function tests showing an obstructive pattern in addition to the typical restrictive pattern in a patient with sarcoidosis. With diseases of the large airways more commonly seen in daily practice, it is important that radiologists be familiar with the appearances, differential diagnoses, and clinical implications of these entities.

Congenital Abnormalities

Congenital airway abnormalities are uncommon and can be associated with cardiovascular and other malformations [1, 3, 8]. Most are asymptomatic and detected incidentally. Congenital tracheal stenosis, tracheoesophageal fistulas (TEFs), and others abnormalities manifest during infancy or childhood, and tracheal atresia is incompatible with life [1, 3, 8].

Although chest radiography occasionally depicts congenital anomalies, CT delineates the exact airway anatomy and easily establishes the diagnosis [1, 5]. Virtual bronchoscopy and other multiplanar 2D and 3D CT reconstruction techniques can be helpful to better characterize congenital airway abnormalities [5].

Tracheal Bronchus

A tracheal bronchus was originally described as a right upper lobe bronchus originating from the trachea (Fig. 1). In the recent literature, the term "tracheal bronchus" has been used for a variety of bronchial anomalies arising from the trachea or a mainstem bronchus that are directed toward an upper lobe [9]. Most tracheal bronchi occur to the right, and they are displaced bronchi rather than supernumerary bronchi [9]. Displacement of the entire right upper lobe bronchus is called "pig bronchus" [1, 8]. Tracheal bronchi are frequently asymptomatic and are incidental imaging findings, but impaired drainage may cause recurrent pneumonia [1, 8]. Endobronchial intubation may occlude a tracheal bronchus, resulting in atelectasis [1].

Accessory Cardiac Bronchus

A cardiac bronchus is a supernumerary bronchus arising from the medial aspect of the bronchus intermedius or, less commonly, the right mainstem bronchus [9] (Fig. 2). This

bronchus progresses conically in an inferior direction toward the pericardium [9]. Most cardiac bronchi end blindly, but some develop into a series of small bronchioles ending in vestigial bronchiolar parenchyma or a ventilated lobulus [8, 10]. Like most other congenital airway abnormalities, cardiac bronchi are typically asymptomatic and are found incidentally on CT examinations, but hemoptysis and recurrent pneumonia may develop in a few patients [8, 10].

Bronchial Atresia

Bronchial atresia is the congenital obliteration of a bronchial segment—most frequently the left upper lobe—with normal development of airways proximal and distal to the lesion [8, 11] (Fig. 3). The airways distal to the obliteration are characteristically dilated and filled with mucus, representing a bronchocele [8, 11]. Bronchial atresia may be accompanied by other abnormalities including bronchogenic cysts, and anomalous branching of the bronchial tree and vascular structures [12]. A characteristic appearance on chest radiography and CT is a central V- or Y-shaped tubular opacity surrounded by hyperlucency due to air trapping and hypoperfusion [8, 11]. The area of hyperlucency can be better seen on expiratory CT scans but may be missing or replaced by atelectasis in the absence of collateral ventilation [8].

Tracheoesophageal Fistula

TEF is defined as an abnormal connection between the trachea and the esophagus (Fig. 4). Most congenital TEFs occur with esophageal atresia and are diagnosed in neonates [13]. TEFs without esophageal atresia are also referred to as "H-type fistulas" and may occasionally be diagnosed later in life [14]. TEFs in adults are most frequently acquired because of tumors, infection, or trauma [15]. Congenital TEFs have a high association with other congenital anomalies, including cardiovascular, genitourinary, and gastrointestinal malformations [13, 16, 17].

On chest radiography, a TEF may be suspected if there is an unusual amount of intestinal distention from air leaking into the gastrointestinal tract [18]. Radiographic contrast studies of the esophagus may show a TEF [19], but at times CT may be required for this purpose [20, 21].

Tracheal Stenosis

Congenital stenosis refers to narrowing of the tracheal lumen without airway wall thickening and is most frequently caused by complete or near-complete tracheal rings [1, 8] (Fig. 5). Severe congenital tracheal stenosis involving long airway segments typically becomes symptomatic early during infancy [1]. Mild congenital stenosis may be asymptomatic and an incidental finding in adults [1]. The typical imaging appearance is diffuse, segmental, or funnellike progressive airway stenosis without wall thickening [1, 8]. Long segmental stenosis due to complete tracheal rings may be associated with a left pulmonary artery sling [8, 22]. Tracheal stenosis, which is associated with a high mortality, is treated with bronchoscopic dilatation and stent placement, surgical resection of the involved segments, or tracheoplasty [8, 23].

Iatrogenic and Traumatic Abnormalities

Postintubation Stenosis

Endotracheal intubation and tracheostomy are the most common causes of acquired focal tracheal stenosis [1, 24] (Fig. 6). High cuff pressure causes ischemic necrosis of the mucosa, followed by scarring and stenosis, which typically occurs 3–4 cm below the cricoid cartilage [24]. Stenosis also can occur more cranially at the site of tracheostomy. Careful inspection of the trachea on chest radiography can reveal focal luminal narrowing [24, 25]. CT detects the characteristic circumferential hourglass stenosis, which is better seen on coronal and sagittal reformations than on axial images [1, 5, 25]. In acute stenosis, edema and granulation tissue may appear as concentric or eccentric soft-tissue thickening. In chronic stenosis, thickening is minimal, but weakening of airway cartilage may lead to focal expiratory airway collapse on dynamic CT [26].

Iatrogenic airway stenosis can also follow lung transplant at the site of anastomosis, typically developing within 9 months after surgery [25, 27]. Another posttransplant complication is anastomotic dehiscence, which may manifest with pneumomediastinum and pneumothorax [25, 27, 28].

Traumatic Injury

Traumatic rupture of a large airway is uncommon [29–31] (Fig. 7). Most frequently, the bronchi within 2.5 cm of the carina are involved [32]. On chest radiography, pneumomediastinum and pneumothorax from air leaks are common, but nonspecific, findings [29, 30, 33]. The pneumothorax often persists despite chest tube placement [29]. CT can show the site of airway injury as a focal defect or deformity or as the circumferential absence of the airway wall [34, 35]. However, small lesions with intact adventitia and no air leak may be difficult to detect even on CT [34]. A diagnostic, but rare, sign of bronchial disruption is the displacement of collapsed lung in a peripheral and dependent position (fallen lung sign) [35–37]. An extraluminal position of the endobronchial tube or overinflation of its cuff is also indicative of airway injury [34, 35].

Foreign Body Aspiration

Aspiration of a foreign body can result in serious respiratory symptoms, particularly in children [38] (Fig. 8). Generally located in a right bronchus, most foreign bodies are nonopaque food particles that cannot be detected on chest radiography [38–40]. CT can lead to prompt diagnosis by showing and localizing both opaque and nonopaque foreign bodies [41]. Additional imaging findings include atelectasis and air trapping, which is enhanced on dynamic CT sequences [5, 40].

Extrinsic Compression

The large airways can be compressed by enlargement of the surrounding structures, such as the thyroid, esophagus, thymus, lymph nodes, and vessels [15] (Fig. 9). However, airway compression can also be caused by congenital vascular anomalies or fibrosing mediastinitis [42–44]. On chest radiography and CT, extrinsic compression appears as luminal narrowing. In addition to depicting luminal narrowing, CT can reveal the structure compressing the airway. Dynamic CT may show air trapping and acquired focal airway collapse, which can persist after the compression has been treated [45].

Chronic Inflammatory and Infiltrative Diseases

Tracheobronchomalacia

Tracheobronchomalacia refers to excessive airway collapse during expiration (Fig. 10). The collapse is the result of weakening of the airway cartilage [45, 46]. Without weakening of the airway cartilage, airway collapse can be caused by impairment of the posterior longitudinal elastic fibers. In this case, only anterior bulging of the posterior membrane occurs. This finding is referred to as "excessive dynamic airway collapse" (EDAC) [7]. Tracheobronchomalacia can be diffuse or localized [46]. It can be congenital or acquired. The congenital form is usually self-limiting within the first 2 years of life [45]. The acquired form is associated with recurrent in-

American Journal of Roentgenology 2015.205:41-56.

TABLE 1: CT Findings in Chronic Inflammatory and Infiltrative Diseases of the Large Airways

Diseases	CT Findings					
	Lumen	Calcifications	Sparing of the Posterior Membrane	Nodules	Airway Collapse	Additional Findings
Tracheobronchomalacia	N	—	—	—	+++	
Amyloidosis	N	++	—	+	—	
Sarcoidosis	N	+	—	+	—	Predominantly affects bronchi; extrinsic narrowing from enlarged lymph nodes; traction bronchiectasis
Granulomatosis with polyangiitis	N	+	—	+	—	Predominantly affects upper trachea
Relapsing polychondritis	N	++	+++	—	++	
Tracheobronchopathia osteochondroplastica	N	+++	+++	+++	—	
Tracheobronchomegaly	W	—	—	—	++	Small diverticula; bronchiectasis
Bronchial anthracofibrosis	N	—	—	—	—	
Broncholithiasis	N	+++	—	—	—	Calcified lymph nodes

Note—Dash (—) indicates not present, + indicates occasionally present, ++ indicates frequently present, and +++ indicates pathognomonic. N = narrowing, W = widening.

American Journal of Roentgenology 2015.205:41-56.

fection or chronic inflammation in chronic obstructive pulmonary disease (COPD), asthma, cystic fibrosis, and relapsing polychondritis. It has also been associated with endobronchial intubation, tracheostomy, mechanical ventilation, lung transplant, and airway compression [45, 46]. EDAC is likely the result of peripheral airway obstruction and inflammation in patients with COPD and asthma and is associated with morbid obesity [7].

Both tracheobronchomalacia and EDAC are increasingly recognized as a common cause of nonspecific respiratory symptoms, such as cough, dyspnea, wheezing, sputum production, and recurrent infections [46]. The traditional diagnosis is based on the bronchoscopic decrease in tracheal diameter of more than 50% during expiration [6, 45, 46]. Dynamic CT studies, however, have shown that airway collapse exceeding 50% with forced expiration is present in many healthy individuals [47–49]. Therefore, investigators have proposed the use of a cutoff of at least 70% collapse of the airway on CT to avoid overdiagnosing airway collapse [6, 46, 47].

On chest radiography and CT performed during inspiration, the trachea shows a normal rounded or, sometimes, a lunate configuration, with a ratio of the coronal to sagittal diameter of more than 1 [47, 50]. This lunate configuration should not be confused with saber-sheath trachea, occurring in COPD, in which the ratio of the coronal to sagittal diameter is less than two thirds [15, 51]. However, dynamic CT sequences with active respiratory maneuvers are required to diagnose airway collapse [1, 45, 46]. There are two classic patterns of collapse: crescentic and circumferential [46, 47]. The crescentic pattern shows marked anterior bulging of the posterior membrane and is also known as the "frown" sign [50]. In the circumferential pattern, the collapse is more evenly distributed [46]. Airway collapse is frequently accompanied by air trapping [45, 46].

Progressive airway collapse can cause severe respiratory distress, which can be treated with continuous positive airway pressure, stent placement, and tracheoplasty [45, 46].

Amyloidosis

Amyloidosis is characterized by the extracellular accumulation of abnormal proteinaceous, insoluble fibrils [52, 53]. These fibrils disrupt the underlying bronchial architecture, act as space-occupying masses, and may have cytotoxic effects [52]. In systemic amyloidosis, involvement of the respiratory tract is frequent but is typically asymptomatic and is an incidental finding [54]. Localized amyloidosis of the respiratory tract is rare [54–56] (Fig. 11). It can manifest as submucosal tracheobronchial deposits, solitary or multiple pulmonary nodules, and diffuse pulmonary interstitial deposits [55–57]. Tracheobronchial amyloidosis is the most frequent form and involves the large airways diffusely. Occasionally, amyloid deposits cause unifocal or nodular disease, thus mimicking endobronchial neoplasms [53]. Tracheobronchial amyloidosis typically presents with nonspecific symptoms such as cough, exertional dyspnea, wheezing, and mild hemoptysis [58, 59].

Diffuse or focal accumulation of amyloid causes irregular mural thickening and luminal narrowing, which may result in secondary obstructive hyperinflation, atelectasis, or recurrent pneumonia [58–60]. Amyloidosis is best detected on CT, which also may show a solitary nodule or multiple nodules protruding into the airway lumen [58–60]. CT may detect mural calcifications, which should not be confused with tracheobronchopathia osteochondroplastica. In tracheobronchopathia osteochondroplastica, the posterior membranous wall of the trachea is typically spared unlike the circumferential pattern in amyloidosis [3, 25].

Tracheobronchial amyloidosis often progresses to respiratory distress, with one third of patients dying of pneumonia or respiratory insufficiency [57, 58]. Treatment options include bronchoscopic techniques, such as débridement, laser ablation, balloon dilatation, and stent placement [9]. In some patients, local radiation and systemic chemotherapy may be beneficial [52, 58, 59].

Sarcoidosis

Sarcoidosis is an idiopathic multisystemic granulomatous disease that typically involves thoracic lymph nodes and the lung parenchyma [61, 62]. Involvement of the trachea and main bronchi is rare, whereas abnormalities in the lobar and segmental bronchi are more common [63, 64] (Fig. 12). In the early stage, airway abnormalities consist of mucosal and submucosal inflammation and noncaseating granulomas, which cause smooth, irregular, or nodular luminal narrowing. Later stage abnormalities include fibrotic parenchymal changes that distort the airways and cause traction bronchiectasis [62, 65]. Airway sarcoidosis presents with

nonspecific clinical signs. In patients with severe involvement, mechanical airway obstruction may cause coughing, wheezing, and pulmonary function test results suggestive of an obstruction [61, 62, 65].

Severe narrowing of the trachea or main bronchi can occasionally be seen on chest radiography. However, CT can detect subtle airway lesions, such as nodular or smooth airway wall thickening and narrowing, that can result in complete luminal stenosis [65–67] (Table 1). Airway narrowing may also result from enlarged lymph nodes compressing the airway [67]. Coexisting parenchymal fibrosis may cause airway distortion and traction bronchiectasis [62, 67]. Traction bronchiectasis reflects the severity of the fibrosis and, along with concomitant signs of airways disease, can be helpful in monitoring disease progression and response to treatment [62, 65, 68].

Granulomatosis With Polyangiitis

Granulomatosis with polyangiitis (GPA) is an antineutrophil cytoplasmic antibody–associated vasculitis [69]. Characterized by necrotizing granulomas and vasculitis, GPA primarily affects small and medium-sized vessels [70]. Up to half of patients with GPA have tracheobronchial tree involvement, which rarely is the only manifestation of the disease [69].

In large airway GPA, acute inflammatory mucosal abnormalities range from edema to ulcers. These abnormalities commonly cause airway wall thickening and fixed or reversible stenosis, often of the upper trachea [69] (Fig. 13). Chest radiography may show a smooth stenosis of the airways and pulmonary opacities that indicate lung involvement. On CT, signs of large airway involvement include smooth or nodular circumferential thickening of the tracheobronchial wall that leads to a single stenosis or multiple stenoses [70–72] (Table 1). Irregular calcifications of the tracheal cartilage rings and bronchiectasis can occur [70–72]. Severe airway obstruction may lead to atelectasis. Pulmonary involvement produces parenchymal consolidations with ground-glass halos, nodules, and masses that often cavitate [70–72].

Treatment with immunosuppressive drugs has substantially improved the prognosis of GPA, although there is potential for relapse [69]. If airway obstruction persists, dilatation, stent placement, laser ablation, tracheostomy, or surgical resection can improve symptoms [69].

Relapsing Polychondritis

Relapsing polychondritis is a rare autoimmune disorder causing recurrent inflammation and subsequent destruction of cartilage in the ear, joints, airways, and nose [73, 74]. The destroyed cartilage is then replaced by granulomatous tissue or fibrosis [73, 74].

Up to 50% of patients with relapsing polychondritis have airway disease, which can occur anytime during its course and is typically diffuse [73–75] (Fig. 14). Inflammation and destruction of the airway cartilage lead to the loss of its supportive function, causing excessive collapse of the airways during expiration [73, 76]. Other airway abnormalities are stenosis due to mural thickening and obstructive bronchiectasis [73]. CT shows diffuse smooth thickening of the tracheobronchial wall with characteristic sparing of the posterior membranous part (Table 1). Calcifications, stenosis, and obstructive bronchiectasis can also occur [15, 26, 73]. Dynamic CT can show excessive collapsibility, which is often associated with air trapping [76].

Patients with severe airway involvement have a poor prognosis [77]. Early detection and treatment are crucial to delay destruction of cartilage [75]. Continued positive airway pressure, various types of bronchoscopic intervention such as laser therapy, balloon dilatation, and stenting, and tracheostomy in severe stenosis of the upper trachea can improve the symptoms related to airway involvement [73–75].

Tracheobronchomegaly

Tracheobronchomegaly, or Mounier-Kuhn syndrome, refers to the marked dilatation of the trachea and main bronchi that results from atrophy of smooth muscle and elastic tissue in the airway walls [15, 78, 79] (Fig. 15). This disorder of unknown cause may result from a congenital predisposition combined with acquired factors such as infections and chronic irritation from smoking [78, 79]. The most frequent clinical complaint related to tracheobronchomegaly is recurrent airway infections due to retained secretions [78]. However, chest radiography may suggest tracheobronchomegaly in asymptomatic patients undergoing imaging for other indications [15, 78]. CT permits precise determination of the increased diameter and extent of airway dilatation [1, 15] (Table 1). In women with tracheobronchomegaly, the coronal diameter of the trachea exceeds 21 mm and the sagittal diameter is greater than 23 mm. In men, the coronal diameter of the trachea is greater than 25 mm and the sagittal diameter is more than 27 mm [1, 15, 79]. In addition to increased tracheal diameter, CT may show a corrugated airway wall, multiple small diverticula, and bronchiectasis [1, 3, 15]. Dynamic CT sequences commonly show tracheobronchomalacia as increased airway collapsibility [1, 15].

Patients with tracheobronchomegaly are treated supportively with physiotherapy, mucolytic agents, and antibiotics. In severe cases, airway stenting or tracheoplasty may improve the quality of life [78].

Tracheobronchopathia Osteochondroplastica

Tracheobronchopathia osteochondroplastica is a rare idiopathic condition that causes thickening of the tracheal rings and multiple sessile osteochondral nodules in the submucosa of the large airways [80] (Fig. 16). The nodules are connected to the perichondrium of the tracheal rings and protrude into the airway lumen [25, 80]. Tracheobronchopathia osteochondroplastica most commonly affects the trachea, but all airways with cartilaginous components can be involved [25, 80, 81]. Most patients are asymptomatic and experience a benign disease with only minimal progression [80].

Chest radiography often shows normal findings but can show tracheal scalloping or irregular asymmetric airway stenosis [28]. On CT, thickened cartilage rings with irregular calcifications and multiple nodules are pathognomonic for tracheobronchopathia osteochondroplastica [3, 25] (Table 1). The nodules project into the airway lumen from the anterior and lateral wall and can be calcified. The posterior membrane of the trachea is spared because of the absence of cartilaginous tissue [3, 25, 80]. Atelectasis and pneumonia can be complications of tracheobronchopathia osteochondroplastica seen on imaging [80].

Bronchial Anthracofibrosis

Bronchial anthracofibrosis is characterized by focal luminal narrowing of the bronchi with darkened bronchial mucosa in patients without exposure to coal dust or cigarette smoking [82] (Fig. 17). Suggested causes of this condition are tuberculosis and, more recently, chronic exposure to biomass smoke [82–85]. The airway narrowing is smooth, is frequently multifocal, and has a predilection for the right upper and middle lobe bronchi [82–84]. Pathology reveals anthracotic pigment within the bronchial mucosa and dense fibrotic changes in involved tissue [82]. Patients present with nonspecific symptoms such as cough, increased sputum production, dyspnea, and recurrent infection [82, 83].

Chest radiography does not show the luminal narrowing but can show consolidations or

American Journal of Roentgenology 2015.205:41-56.

atelectasis [82, 83]. On CT, bronchial narrowing is typically smooth and is caused by thickening of the bronchial walls and peribronchial soft tissues [82, 84] (Table 1). In addition to the airway lesions, lymph nodes surrounding the affected bronchi are often enlarged and may be calcified [82–84]. Consolidations and atelectasis are common in portions of the lung distal to the site of airway narrowing [82, 84]. The appearance of anthracofibrosis can simulate bronchogenic carcinoma and endobronchial tuberculosis [83]. The bronchial narrowing in anthracofibrosis is smooth and is frequently multifocal, whereas there is a more nodular pattern that typically is confined to one site in bronchogenic carcinoma [83]. Nevertheless, a definite diagnosis of anthracofibrosis requires bronchoscopy and bronchial biopsy [83]. If anthracofibrosis is associated with active tuberculosis, treatment of the infection may decrease airway narrowing [82].

Broncholithiasis

Broncholithiasis refers to calcified material within the bronchial lumen (Fig. 18). The calcified material most commonly is a calcified lymph node, which is typically caused by necrotizing granulomatous lymphangitis from histoplasmosis or tuberculosis [86, 87]. At times, calcified nodes compressing a bronchus are also considered to be broncholiths [86].

The disappearance of or a change in the position of a previously seen calcified opacity on chest radiography suggests broncholithiasis [87]. CT is more sensitive for making the diagnosis by showing calcified material within or compressing a bronchus [87] (Table 1). Additional imaging findings are bronchiectasis, obstructive atelectasis, and multiple calcified lymph nodes [87]. Dynamic CT may show postobstructive air trapping [87].

Infection

Infection of the large airways can be caused by a variety of pathogens [2, 15, 88]. Infections lead to an inflammatory response that results in nonspecific focal or diffuse airway wall thickening and occasionally in luminal narrowing [88–91].

Viral

Viral croup is a common cause of upper respiratory tract obstruction and severe respiratory symptoms in children [92–94]. Mucosal swelling of the upper airways causes a characteristic seallike barking cough, stridor, and hoarseness [92–94]. The diagnosis of croup is made clinically, and chest radiography is indicated only when the cause is clinically uncertain [92–94]. A typical appearance in croup is an inverted V–like narrowing of the upper trachea on frontal views (steeple sign) without involvement of the epiglottis [95].

Bacterial

Bacterial tracheitis, also referred to as "laryngotracheobronchitis" and "bacterial croup" or "membranous croup," is a rare, but severe, large airway infection that is characterized by membranous tracheal secretions [93]. The clinical presentation of bacterial tracheitis is similar to that of severe viral croup, with cough, stridor, and hoarseness [93, 96]. There also may be signs of lower respiratory tract involvement, such as crackles, wheezing, and pneumonia [93]. Chest radiography shows typical crouplike narrowing of the upper trachea, but there often are also irregular, linear opacities within the tracheal lumen representing membranous tracheal secretions [97]. This potentially life-threating condition is treated with antibiotics, and endobronchial intubation is often performed to prevent complete occlusion of the airways by the secretions [93, 94].

Endobronchial tuberculosis is characterized by wall thickening and luminal narrowing of the large airways due to *Mycobacterium tuberculosis* [3, 15] (Fig. 19). Typically it affects multiple sites within the large airways, most commonly the distal trachea and proximal bronchi [3]. Chest radiography may show luminal narrowing of the large airways or atelectasis [3]. CT may distinguish between the active and fibrotic stages, which may coexist [3, 15, 98]. The active reversible stage of endobronchial tuberculosis presents as irregular luminal narrowing with contrast-enhancing thickening of the airway wall [3, 15, 98]. The irreversible fibrotic stage manifests as smooth narrowing with only minimal wall thickening [3, 15, 98]. Other abnormalities on CT include lymphadenopathy, which can compress the large airways, bronchiectasis, and parenchymal inflammatory changes [15]. If there is severe stenosis, bronchoscopic dilatation and stenting may be indicated [15].

Rhinoscleroma is a chronic progressive granulomatous infection of the nose caused by *Klebsiella rhinoscleromatis* [15, 99]. Endemic in parts of Africa, Latin America, and Eastern Europe, rhinoscleroma is rare in the United States [99]. Typical signs of rhinoscleroma include chronic nasal obstruction, rhinorrhea, epistaxis, absence of the uvula, and nasal deformities (termed "Hebra nose"). Dyspnea and stridor suggest airway lesions, such as granulomatous nodules, and dense fibrotic stenosis [99, 100]. Chest radiography may show nodular irregularities or diffuse narrowing of the large airways [28]. On CT, large airway rhinoscleroma appears as irregular, nodular, and concentric luminal narrowing with airway wall thickening of soft-tissue attenuation without calcifications [25, 100]. At times, the airway mucosa shows crypt or sinuslike lesions [100]. This slowly progressing entity is treated with a prolonged course of antibiotics, but recurrence is common [99]. Airway abnormalities are best treated with bronchoscopic dilatation and laser ablation [99].

Fungal

Fungal species that infect the trachea or bronchi include *Aspergillus, Coccidioides*, *Candida*, *Cryptococcus*, and *Histoplasma* organisms [15, 101] (Fig. 20). Up to 80% of patients with a fungal infection of the tracheobronchial tree have an underlying condition that compromises their immune system [101]. Depending on a patient's immunocompetence, *Aspergillus* infection may manifest as allergic bronchopulmonary aspergillosis, intrabronchial aspergilloma, semiinvasive necrotizing bronchial aspergillosis, or invasive acute tracheobronchitis. Allergic bronchopulmonary aspergillosis is a hypersensitivity reaction to *Aspergillus* organisms in patients with asthma or cystic fibrosis. Excessive mucus production and ciliary dysfunction lead to mucoid impaction without mucosal invasion [102].

Chest radiography may not show the airway abnormalities [101, 102]. CT typically shows intraluminal nodules or masses of soft-tissue attenuation in the tracheobronchial tree, airway wall thickening, airway stenosis, and occasionally intramural air [101–103]. Bronchiectasis or airway compression from lymphadenopathy may be present [3, 101]. In allergic bronchopulmonary aspergillosis, fingerlike opacities of soft-tissue attenuation are a sign of mucoid impaction and bronchiectasis [102].

Although imaging can be suggestive of airway mycosis, a definite diagnosis is typically made by fungal cultures obtained at bronchoscopy [101]. Fungal airway lesions are treated bronchoscopically, with vaporization or excision of luminal nodules and dilatation and stent placement for airway stenosis [101].

Neoplasms

Benign neoplasms account for less than 10% of airway neoplasms [104]. The most frequent benign neoplasms are hamartomas,

American Journal of Roentgenology 2015.205:41-56.

which nevertheless are uncommon lesions, and tracheobronchial papillomatoses [104]. Tracheobronchial papillomatosis is caused by human papillomavirus and predominantly involves the larynx (Fig. 21). However, it may spread to the trachea; the bronchi; and, rarely, the lung. In the trachea and bronchi, tracheobronchial papillomatosis presents as multiple nodules projecting into the airway lumen or as diffuse nodular wall thickening [2, 104]. Tracheobronchial papillomatosis that has spread to the lung manifests as multiple bilateral cysts and nodules. The nodules are often cavitated [2]. Less frequent benign neoplasms are leiomyomas, lipomas, chondromas, and neurogenic tumors [104]. Benign neoplasms are typically well-defined, round, smooth lesions that are smaller than 2 cm in diameter and do not invade the airway wall [1, 3, 105].

Malignant neoplasms of the large airways are more common than benign neoplasms [104]. Most reflect direct invasion by adjacent thyroid, laryngeal, esophageal, or lung cancer [104]. Less frequent are primary malignant neoplasms and metastases from breast, colorectal, and renal carcinomas or melanoma [104] (Fig. 22). In the trachea, the predominant types of primary malignant neoplasms are squamous cell carcinoma and adenoid cystic carcinoma [106]. Squamous cell carcinomas are aggressive neoplasms associated with smoking, with a peak incidence between the ages of 50 and 70 years [2, 104, 106]. Adenoid cystic carcinoma has its peak incidence at a younger age, has a more prolonged course, and recurs locally [2, 104, 106] (Fig. 23). In the bronchi, the predominant types of malignant neoplasms are bronchial squamous cell carcinoma, small cell carcinoma, carcinoid tumor (Fig. 24), and mucoepidermoid carcinoma [2]. Malignant neoplasms tend to be flat or polypoid lesions that are larger than 2 cm and have lobulated or irregular borders [1]. Advanced malignant neoplasms extend outside the large airways and invade mediastinal structures [1].

Chest radiography may show focal luminal narrowing from a soft-tissue opacity or signs of airway obstruction such as atelectasis and recurrent pneumonia [28]. CT shows an intraluminal mass of soft-tissue attenuation that may extend through the tracheal wall and invade surrounding structures. The presence of fat and cartilaginous tissue within a lesion on CT indicates a hamartoma [2, 3], although other fat-containing lesions include lipoma and well-differentiated liposarcoma [1, 3]. Calcifications and marked homogeneous contrast enhancement due to hypervascularity suggest carcinoid tumor [1, 3, 107]. Nonspherical carcinoid tumors with an elongated shape often have a long axis oriented parallel to the adjacent airway [107]. A definitive diagnosis, however, is made by biopsy [1].

Surgical resection is the preferred treatment of all airway neoplasms [1, 106]. Radiation may be beneficial in patients with unresectable disease or as an adjunctive therapy to surgery [1, 106].

Conclusion

In this article, we have discussed the appearance, clinical implications, and differential diagnoses of the most common disorders affecting the large airways. A standardized evaluation of the large airways includes assessment of the lumen, wall structure and wall thickness, and the surrounding soft tissues and lung parenchyma. There are distinct patterns of dimensional and structural changes of these components that are characteristic of individual airways diseases. The radiologic patterns described in this article will help radiologists in their diagnostic approach to large airways diseases.

Acknowledgments

We thank Pierluigi Ciet (Erasmus Medical Center, Rotterdam, The Netherlands) for Figures 4 and 5, Jorge A. Soto (Boston Medical Center, Boston, MA) for Figure 7, Kyung Soo Lee (Samsung Medical Center, Seoul, Korea) for Figure 17, and Jin Mo Goo (Seoul National University College of Medicine, Seoul, Korea) for Figure 19.

References

1. Boiselle PM. Imaging of the large airways. *Clin Chest Med* 2008; 29:181–193
2. Ngo AV, Walker CM, Chung JH, et al. Tumors and tumorlike conditions of the large airways. *AJR* 2013; 201:301–313
3. Kang EY. Large airway diseases. *J Thorac Imaging* 2011; 26:249–262
4. Hyde DM, Hamid Q, Irvin CG. Anatomy, pathology, and physiology of the tracheobronchial tree: emphasis on the distal airways. *J Allergy Clin Immunol* 2009; 124(suppl 6):S72–S77
5. Lee KS, Boiselle PM. Update on multidetector computed tomography imaging of the airways. *J Thorac Imaging* 2010; 25:112–124
6. Lee EY, Litmanovich D, Boiselle PM, Multidetector CT: evaluation of tracheobronchomalacia. *Radiol Clin North Am* 2009; 47:261–269
7. Murgu S, Colt H. Tracheobronchomalacia and excessive dynamic airway collapse. *Clin Chest Med* 2013; 34:527–555
8. Desir A, Ghaye B. Congenital abnormalities of intrathoracic airways. *Radiol Clin North Am* 2009; 47:203–225
9. Ghaye B, Szapiro D, Fanchamps JM, Dondelinger RF. Congenital bronchial abnormalities revisited. *RadioGraphics* 2001; 21:105–119
10. Ghaye B, Kos X, Dondelinger RF. Accessory cardiac bronchus: 3D CT demonstration in nine cases. *Eur Radiol* 1999; 9:45–48
11. Nemec SF, Bankier AA, Eisenberg RL. Pulmonary hyperlucency in adults. *AJR* 2013; 200:[web]W101–W115
12. Wang YQ, Dai WM, Sun Y, Chu XY, Yang B, Zhao M. Congenital bronchial atresia: diagnosis and treatment. *Int J Med Sci* 2012; 9:207–212
13. Sharma AK, Shekhawat NS, Agrawal LD, Chaturvedi V, Kothari SK, Goel D. Esophageal atresia and tracheoesophageal fistula: a review of 25 years' experience. *Pediatr Surg Int* 2000; 16:478–482
14. Zacharias J, Genc O, Goldstraw P. Congenital tracheoesophageal fistulas presenting in adults: presentation of two cases and a synopsis of the literature. *J Thorac Cardiovasc Surg* 2004; 128:316–318
15. Hansell DM, Lynch DA, McAdams HP, Bankier AA. Disease of the airways. In: Hansell DM, Lynch DA, McAdams HP, Bankier AA. *Imaging of diseases of the chest*, 5th ed. New York, NY: Mosby Elsevier, 2010:715–786
16. Depaepe A, Dolk H, Lechat MF. The epidemiology of tracheo-oesophageal fistula and oesophageal atresia in Europe: EUROCAT Working Group. *Arch Dis Child* 1993; 68:743–748
17. Shaw-Smith C. Oesophageal atresia, tracheo-oesophageal fistula, and the VACTERL association: review of genetics and epidemiology. *J Med Genet* 2006; 43:545–554
18. Thomas PS, Chrispin AR. Congenital tracheo-oesophageal fistula without oesophageal atresia. *Clin Radiol* 1969; 20:371–374
19. Laffan EE, Daneman A, Ein SH, Kerrigan D, Manson DE. Tracheoesophageal fistula without esophageal atresia: are pull-back tube esophagograms needed for diagnosis? *Pediatr Radiol* 2006; 36:1141–1147
20. Johnson JF, Sueoka BL, Mulligan ME, Lugo EJ. Tracheoesophageal fistula: diagnosis with CT. *Pediatr Radiol* 1985; 15:134–135
21. Fitoz S, Atasoy C, Yagmurlu A, Akyar S, Erden A, Dindar H. Three-dimensional CT of congenital esophageal atresia and distal tracheoesophageal fistula in neonates: preliminary results. *AJR* 2000; 175:1403–1407
22. Berdon WE. Rings, slings, and other things: vascular compression of the infant trachea updated from the midcentury to the millennium—the

American Journal of Roentgenology 2015.205:41-56.

legacy of Robert E. Gross, MD, and Edward B. D. Neuhauser, MD. *Radiology* 2000; 216:624–632
23. Maeda K, Yasufuku M, Yamamoto T. A new approach to the treatment of congenital tracheal stenosis: balloon tracheoplasty and expandable metallic stenting. *J Pediatr Surg* 2001; 36:1646–1649
24. Wain JC Jr. Postintubation tracheal stenosis. *Semin Thorac Cardiovasc Surg* 2009; 21:284–289
25. Prince JS, Duhamel DR, Levin DL, Harrell JH, Friedman PJ. Nonneoplastic lesions of the tracheobronchial wall: radiologic findings with bronchoscopic correlation. *RadioGraphics* 2002; 22:S215–S230 [Erratum in *RadioGraphics* 2003; 23:191]
26. Webb EM, Elicker BM, Webb WR. Using CT to diagnose nonneoplastic tracheal abnormalities: appearance of the tracheal wall. *AJR* 2000; 174:1315–1321
27. Porhownik NR. Airway complications post lung transplantation. *Curr Opin Pulm Med* 2013; 19:174–180
28. Eisenberg RL. Chest patterns. In: Eisenberg RL, ed. *Clinical imaging: an atlas of differential diagnosis.* Philadelphia, PA: Lippincott Williams & Wilkins, 2010:1–320
29. Stark P. Imaging of tracheobronchial injuries. *J Thorac Imaging* 1995; 10:206–219
30. Chu CPW, Chen PP. Tracheobronchial injury secondary to blunt chest trauma: diagnosis and management. *Anaesth Intensive Care* 2002; 30:145–152
31. Karmy-Jones R, Wood DE. Traumatic injury to the trachea and bronchus. *Thorac Surg Clin* 2007; 17:35–46
32. Prokakis C, Koletsis EN, Dedeilias P, Fligou F, Filos K, Dougenis D. Airway trauma: a review on epidemiology, mechanisms of injury, diagnosis and treatment. *J Cardiothorac Surg* 2014; 9:117
33. Wiot JF. Tracheobronchial trauma. *Semin Roentgenol* 1983; 18:15–22
34. Chen JD, Shanmuganathan K, Mirvis SE, Killeen KL, Dutton RP. Using CT to diagnose tracheal rupture. *AJR* 2001; 176:1273–1280
35. Thoongsuwan N, Kanne JP, Stern EJ. Spectrum of blunt chest injuries. *J Thorac Imaging* 2005; 20:89–97
36. Tack D, Defrance P, Delcour C, Gevenois PA. The CT fallen-lung sign. *Eur Radiol* 2000; 10:719–721
37. Wintermark M, Schnyder P, Wicky S. Blunt traumatic rupture of a mainstem bronchus: spiral CT demonstration of the "fallen lung" sign. *Eur Radiol* 2001; 11:409–411
38. Cataneo AJ, Reibscheid SM, Ruiz Júnior RL, Ferrari GF. Foreign body in the tracheobronchial tree. *Clin Pediatr (Phila)* 1997; 36:701–706
39. Franquet T, Giménez A, Rosón N, Torrubia S, Sabaté JM, Pérez C. Aspiration diseases: findings, pitfalls, and differential diagnosis. *RadioGraphics* 2000; 20:673–685
40. Swanson KL. Airway foreign bodies: what's new? *Semin Respir Crit Care Med* 2004; 25:405–411
41. Zissin R, Shapiro-Feinberg M, Rozenman J, Apter S, Smorjik J, Hertz M. CT findings of the chest in adults with aspirated foreign bodies. *Eur Radiol* 2001; 11:606–611
42. Sebening C, Jakob H, Tochtermann U, et al. Vascular tracheobronchial compression syndromes: experience in surgical treatment and literature review. *Thorac Cardiovasc Surg* 2000; 48:164–174
43. Gross RE. Arterial malformations which cause compression of the trachea or esophagus. *Circulation* 1955; 11:124–134
44. Rossi SE, McAdams HP, Rosado-de-Christenson ML, Franks TJ, Galvin JR. Fibrosing mediastinitis. *RadioGraphics* 2001; 21:737–757
45. Carden KA, Boiselle PM, Waltz DA, Ernst A. Tracheomalacia and tracheobronchomalacia in children and adults: an in-depth review. *Chest* 2005; 127:984–1005
46. Ridge CA, O'Donnell CR, Lee EY, Majid A, Boiselle PM. Tracheobronchomalacia: current concepts and controversies. *J Thorac Imaging* 2011; 26:278–289
47. Boiselle PM, O'Donnell CR, Bankier AA, et al. Tracheal collapsibility in healthy volunteers during forced expiration: assessment with multidetector CT. *Radiology* 2009; 252:255–262
48. Stern EJ, Graham CM, Webb WR, Gamsu G. Normal trachea during forced expiration: dynamic CT measurements. *Radiology* 1993; 187:27–31
49. Litmanovich D, O'Donnell CR, Bankier AA, et al. Bronchial collapsibility at forced expiration in healthy volunteers: assessment with multidetector CT. *Radiology* 2010; 257:560–567
50. Boiselle PM, Ernst A. Tracheal morphology in patients with tracheomalacia: prevalence of inspiratory lunate and expiratory "frown" shapes. *J Thorac Imaging* 2006; 21:190–196
51. Greene R, Lechner GL. "Saber-sheath" trachea: a clinical and functional study of marked coronal narrowing of the intrathoracic trachea. *Radiology* 1975; 115:265–268
52. Gillmore JD, Hawkins PN. Amyloidosis and the respiratory tract. *Thorax* 1999; 54:444–451
53. Berk JL, O'Regan A, Skinner M. Pulmonary and tracheobronchial amyloidosis. *Semin Respir Crit Care Med* 2002; 23:155–165
54. Dahl KA, Kernstine KH, Vannatta TL, Karwal MW, Thomas KW, Schraith DF. Tracheobronchial amyloidosis: a surgical disease with long-term consequences. *J Thorac Cardiovasc Surg* 2004; 128:789–792
55. Thompson PJ, Citron KM. Amyloid and the lower respiratory tract. *Thorax* 1983; 38:84–87
56. Utz JP, Swensen SJ, Gertz MA. Pulmonary amyloidosis: the Mayo Clinic experience from 1980 to 1993. *Ann Intern Med* 1996; 124:407–413
57. Hui AN, Koss MN, Hochholzer L, Wehunt WD. Amyloidosis presenting in the lower respiratory tract: clinicopathologic, radiologic, immunohistochemical, and histochemical studies on 48 cases. *Arch Pathol Lab Med* 1986; 110:212–218
58. O'Regan A, Fenlon HM, Beamis JF, Steele MP, Skinner M, Berk JL. Tracheobronchial amyloidosis: the Boston University experience from 1984 to 1999. *Medicine* 2000; 79:69–79
59. Capizzi SA, Betancourt E, Prakash UBS. Tracheobronchial amyloidosis. *Mayo Clin Proc* 2000; 75:1148–1152
60. Kim HY, Im JG, Song KS, et al. Localized amyloidosis of the respiratory system: CT features. *J Comput Assist Tomogr* 1999; 23:627–631
61. Iannuzzi MC, Rybicki BA, Teirstein AS. Medical progress: sarcoidosis. *N Engl J Med* 2007; 357:2153–2165
62. Hansell DM, Lynch DA, McAdams HP, Bankier AA. Idiopathic diffuse lung disease. In: Hansell DM, Lynch DA, McAdams HP, Bankier AA. *Imaging of diseases of the chest*, 5th ed. New York, NY: Mosby Elsevier, 2010:641–714
63. Morgenthau AS, Teirstein AS. Sarcoidosis of the upper and lower airways. *Expert Rev Respir Med* 2011; 5:823–833
64. Shorr AF, Torrington KG, Hnatiuk OW. Endobronchial biopsy for sarcoidosis: a prospective study. *Chest* 2001; 120:109–114
65. Polychronopoulos VS, Prakash UBS. Airway involvement in sarcoidosis. *Chest* 2009; 136:1371–1380
66. Lenique F, Brauner MW, Grenier P, Battesti JP, Loiseau A, Valeyre D. CT assessment of bronchi in sarcoidosis: endoscopic and pathologic correlations. *Radiology* 1995; 194:419–423
67. Criado E, Sanchez M, Ramirez J, et al. Pulmonary sarcoidosis: typical and atypical manifestations at high-resolution CT with pathologic correlation. *RadioGraphics* 2010; 30:1567–1586
68. Mihailovic-Vucinic V, Jovanovic D. Pulmonary sarcoidosis. *Clin Chest Med* 2008; 29:459–473
69. Polychronopoulos VS, Prakash UBS, Golbin JM, Edell ES, Specks U. Airway involvement in Wegener's granulomatosis. *Rheum Dis Clin North Am* 2007; 33:755–775
70. Nemec SF, Eisenberg RL, Bankier AA. Noninfectious inflammatory lung disease: imaging considerations and clues to differential diagnosis. *AJR* 2013; 201:278–294
71. Lee KS, Kim TS, Fujimoto K, et al. Thoracic manifestation of Wegener's granulomatosis: CT findings in 30 patients. *Eur Radiol* 2003; 13:43–51
72. Aberle DR, Gamsu G, Lynch D. Thoracic manifestations of Wegener granulomatosis: diagnosis and course. *Radiology* 1990; 174:703–709
73. Ernst A, Rafeq S, Boiselle P, et al. Relapsing polychondritis and airway involvement. *Chest*

American Journal of Roentgenology 2015.205:41-56.

2009; 135:1024–1030
74. Kent PD, Michet CJ Jr, Luthra HS. Relapsing polychondritis. *Curr Opin Rheumatol* 2004; 16:56–61
75. Hong G, Kim H. Clinical characteristics and treatment outcomes of patients with relapsing polychondritis with airway involvement. *Clin Rheumatol* 2013; 32:1329–1335
76. Lee KS, Ernst A, Trentham DE, Lunn W, Feller-Kopman DJ, Boiselle PM. Relapsing polychondritis: prevalence of expiratory CT airway abnormalities. *Radiology* 2006; 240:565–573
77. Michet CJ Jr, McKenna CH, Luthra HS, O'Fallon WM. Relapsing polychondritis: survival and predictive role of early disease manifestations. *Ann Intern Med* 1986; 104:74–78
78. Krustins E, Kravale Z, Buls A. Mounier-Kuhn syndrome or congenital tracheobronchomegaly: a literature review. *Respir Med* 2013; 107:1822–1828
79. Woodring JH, Howard RS 2nd, Rehm SR. Congenital tracheobronchomegaly (Mounier-Kuhn syndrome): a report of 10 cases and review of the literature. *J Thorac Imaging* 1991; 6:1–10
80. Abu-Hijleh M, Lee D, Braman SS. Tracheobronchopathia osteochondroplastica: a rare large airway disorder. *Lung* 2008; 186:353–359
81. Leske V, Lazor R, Coetmeur D, et al. Tracheobronchopathia osteochondroplastica: a study of 41 patients. *Medicine* 2001; 80:378–390
82. Chung MP, Lee KS, Han J, et al. Bronchial stenosis due to anthracofibrosis. *Chest* 1998; 113:344–350
83. Gupta A, Shah A. Bronchial anthracofibrosis: an emerging pulmonary disease due to biomass fuel exposure. *Int J Tuberc Lung Dis* 2011; 15:602–612
84. Kim HY, Im JG, Goo JM, et al. Bronchial anthracofibrosis (inflammatory bronchial stenosis with anthracotic pigmentation): CT findings. *AJR* 2000; 174:523–527
85. Kim YJ, Jung CY, Shin HW, Lee BK. Biomass smoke induced bronchial anthracofibrosis: presenting features and clinical course. *Respir Med* 2009; 103:757–765
86. Conces DJ Jr, Tarver RD, Vix VA. Broncholithiasis: CT features in 15 patients. *AJR* 1991; 157:249–253
87. Seo JB, Song KS, Lee JS, et al. Broncholithiasis: review of the causes with radiologic-pathologic correlation. *RadioGraphics* 2002; 22:S199–S213
88. Kwong JS, Müller NL, Miller RR. Diseases of the trachea and main-stem bronchi: correlation of CT with pathologic findings. *RadioGraphics* 1992; 12:645–657
89. Miller WT Jr, Mickus TJ, Barbosa E Jr, Mullin C, Van Deerlin VM, Shiley KT. CT of viral lower respiratory tract infections in adults: comparison among viral organisms and between viral and bacterial infections. *AJR* 2011; 197:1088–1095
90. Marom EM, Goodman PC, McAdams HP. Diffuse abnormalities of the trachea and main bronchi. *AJR* 2001; 176:713–717
91. Marom EM, Goodman PC, McAdams HP. Focal abnormalities of the trachea and main bronchi. *AJR* 2001; 176:707–711
92. Everard ML. Acute bronchiolitis and croup. *Pediatr Clin North Am* 2009; 56:119–133, x–xi
93. Cherry JD. Clinical practice: croup. *N Engl J Med* 2008; 358:384–391
94. Bjornson CL, Johnson DW. Croup. *Lancet* 2008; 371:329–339
95. Salour M. The steeple sign. *Radiology* 2000; 216:428–429
96. Salamone FN, Bobbitt DB, Myer CM, Rutter MJ, Greinwald JH Jr. Bacterial tracheitis reexamined: is there a less severe manifestation? *Otolaryngol Head Neck Surg* 2004; 131:871–876
97. Han BK, Dunbar JS, Striker TW. Membranous laryngotracheobronchitis (membranous croup). *AJR* 1979; 133:53–58
98. Moon WK, Im JG, Yeon KM, Han MC. Tuberculosis of the central airways: CT findings of active and fibrotic disease. *AJR* 1997; 169:649–653
99. Gaafar HA, Gaafar AH, Nour YA. Rhinoscleroma: an updated experience through the last 10 years. *Acta Otolaryngol* 2011; 131:440–446
100. Abou-Seif SG, Baky FA, el-Ebrashy F, Gaafar HA. Scleroma of the upper respiratory passages: a CT study. *J Laryngol Otol* 1991; 105:198–202
101. Karnak D, Avery RK, Gildea TR, Sahoo D, Mehta AC. Endobronchial fungal disease: an underrecognized entity. *Respiration* 2007; 74:88–104
102. Franquet T, Müller NL, Oikonomou A, Flint JD. *Aspergillus* infection of the airways: computed tomography and pathologic findings. *J Comput Assist Tomogr* 2004; 28:10–16
103. Kim KH, Choi YW, Jeon SC, et al. Mucormycosis of the central airways: CT findings in three patients. *J Thorac Imaging* 1999; 14:210–214
104. Park CM, Goo JM, Lee HJ, Kim MA, Lee CH, Kang MJ. Tumors in the tracheobronchial tree: CT and FDG PET features. *RadioGraphics* 2009; 29:55–71
105. Ko JM, Jung JI, Park SH, et al. Benign tumors of the tracheobronchial tree: CT-pathologic correlation. *AJR* 2006; 186:1304–1313
106. Urdaneta AI, Yu JB, Wilson LD. Population based cancer registry analysis of primary tracheal carcinoma. *Am J Clin Oncol* 2011; 34:32–37
107. Chong S, Lee KS, Chung MJ, Han J, Kwon OJ, Kim TS. Neuroendocrine tumors of the lung: clinical, pathologic, and imaging findings. *RadioGraphics* 2006; 26:41–57; discussion, 57–58

American Journal of Roentgenology 2015.205:41-56.

APPENDIX 1: Disorders of the Large Airways

- Congenital abnormalities
  - Tracheal bronchus
  - Accessory cardiac bronchus
  - Bronchial atresia
  - Tracheoesophageal fistula
  - Tracheal stenosis
- Iatrogenic and traumatic abnormalities
  - Postintubation stenosis
  - Traumatic injury
  - Foreign body aspiration
- Extrinsic compression
- Chronic inflammatory and infiltrative diseases
  - Tracheobronchomalacia
  - Amyloidosis
  - Sarcoidosis
  - Granulomatosis with polyangiitis
  - Relapsing polychondritis
  - Tracheobronchomegaly
  - Tracheobronchopathia osteochondroplastica
  - Bronchial anthracofibrosis
  - Broncholithiasis
- Infection
  - Viral
  - Bacterial
  - Fungal
- Neoplasms
  - Benign
    - Hamartoma
    - Respiratory papillomatosis
  - Malignant
    - Squamous cell carcinoma
    - Adenoid cystic carcinoma
    - Carcinoid tumor
    - Mucoepidermoid carcinoma

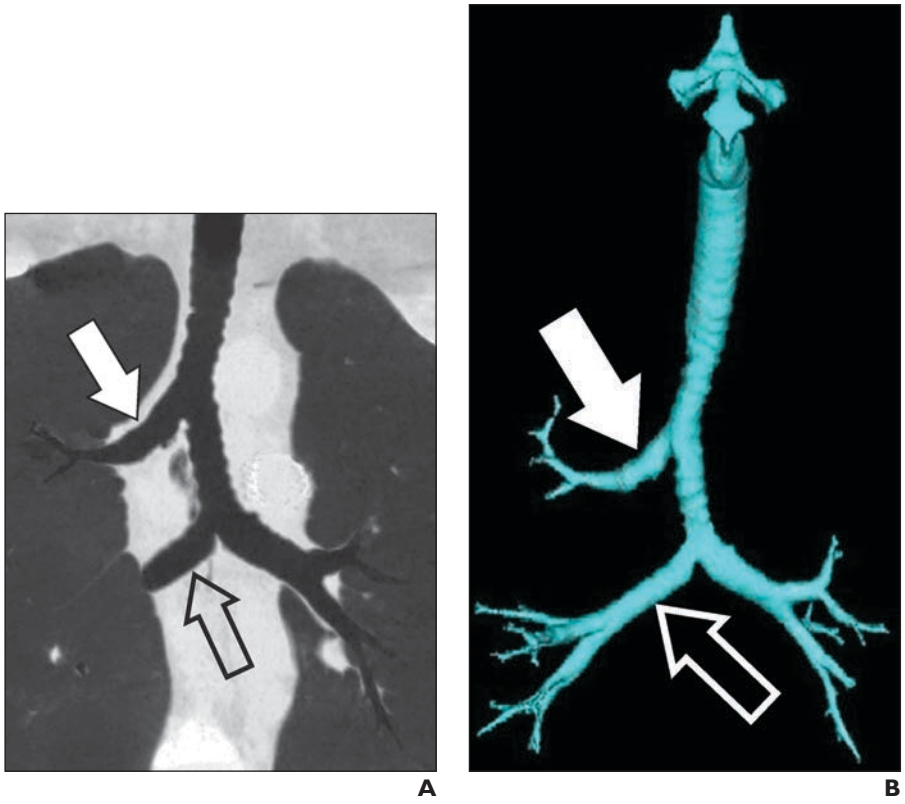

Fig. 1—29-year-old woman with tracheal bronchus. **A** and **B,** Coronal minimum-intensity-projection CT reformation (**A**) and 3D reconstruction (**B**) images of tracheobronchial tree show right upper lobe bronchus (*solid arrow*) arising from trachea instead of right main bronchus (*open arrow*).

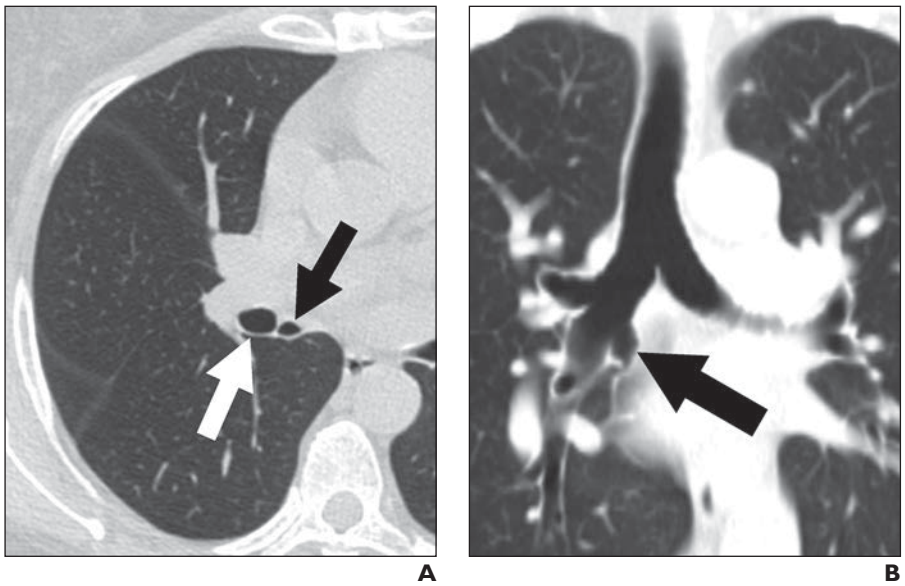

Fig. 2—48-year-old man with cardiac bronchus. **A** and **B,** Axial (**A**) and coronal reformation (**B**) CT images show additional bronchus (*black arrow*) arising from medial aspect of bronchus intermedius (*white arrow*, **A**).

American Journal of Roentgenology 2015.205:41-56.

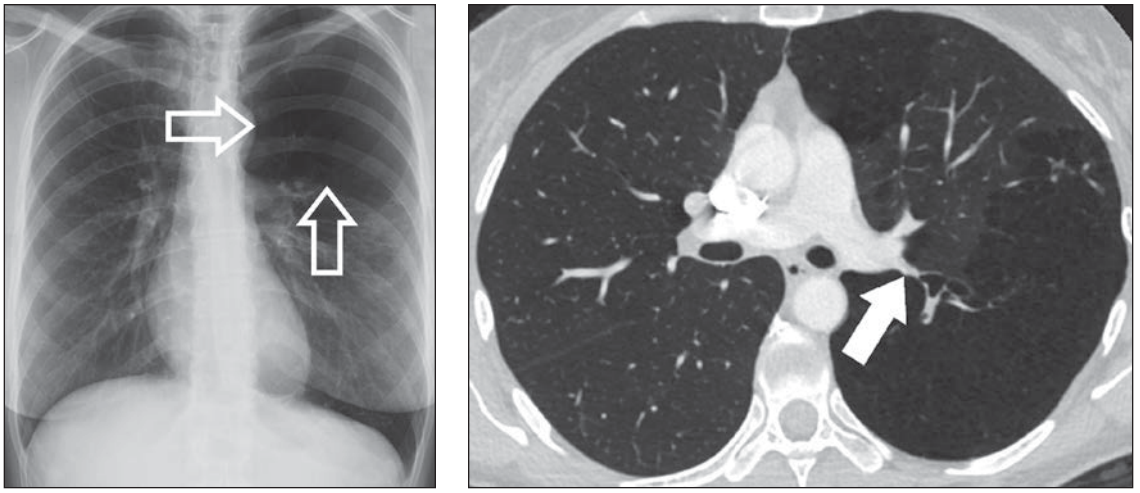

A B

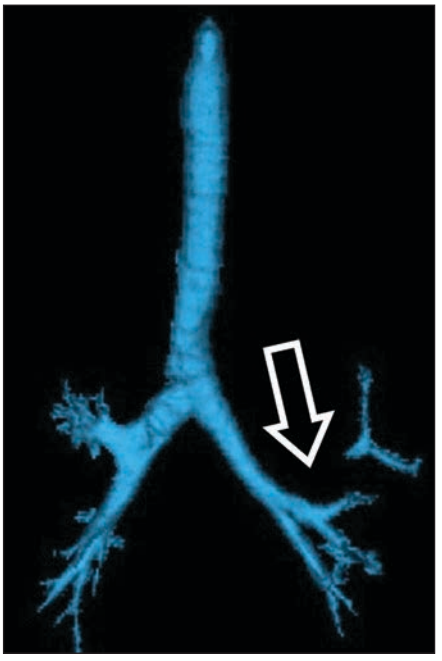

C

Fig. 3—44-year-old woman with bronchial atresia.
A, Posteroanterior chest radiograph shows hyperlucency (*arrows*) of left upper lobe due to decreased vascularity and increased air content.
B, Axial CT image shows atretic bronchial segment (*arrow*) of left upper lobe. Note areas of hyperlucency in lung parenchyma.
C, Three-dimensional reconstruction image of tracheobronchial tree shows atresia (*arrow*) of segment of left upper lobe bronchus.

American Journal of Roentgenology 2015.205:41-56.

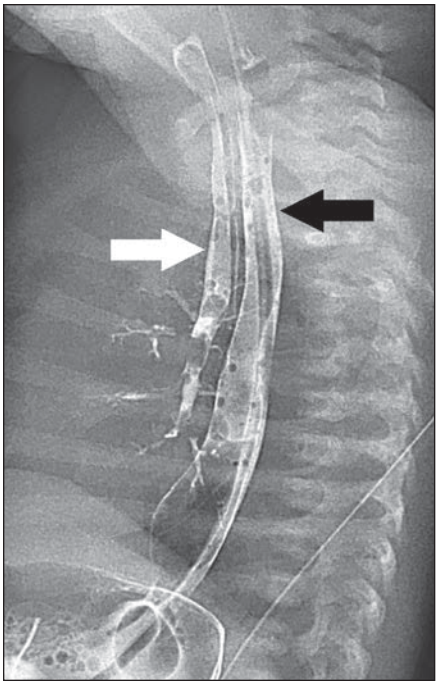

Fig. 4—3-month-old boy with tracheoesophageal fistula. Fluoroscopic image shows contrast-filling of esophagus (*black arrow*) as well as trachea (*white arrow*) due to communication between those two structures. (Courtesy of Ciet P, Erasmus Medical Center, Rotterdam, The Netherlands)

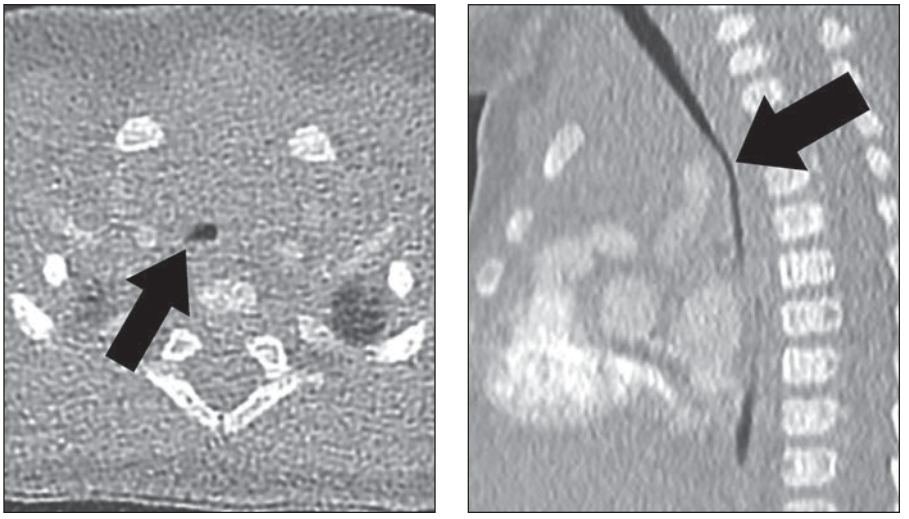

Fig. 5—3-month-old girl with congenital tracheal stenosis. (Courtesy of Ciet P, Erasmus Medical Center, Rotterdam, The Netherlands)
A and **B,** Axial (**A**) and sagittal reformation (**B**) CT images show severe funnel-shaped narrowing of trachea (*arrow*).

Fig. 6—21-year-old woman with postintubation tracheal stenosis. Coronal minimum-intensity-projection CT reformation image shows circumferential hourglasslike narrowing (*arrows*) of trachea.

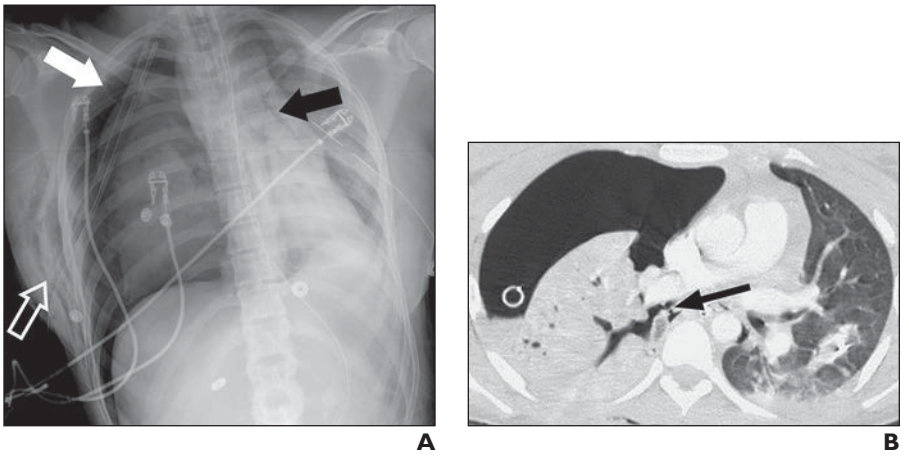

Fig. 7—32-year-old woman with injury of right mainstem bronchus after trauma. (Courtesy of Soto JA, Boston Medical Center, Boston, MA)
A, Anteroposterior chest radiograph shows large right pneumothorax (*solid white arrow*) with mediastinal shift to left accompanied by collapse of right lung, pneumomediastinum (*black arrow*), and emphysema of chest wall (*open arrow*).
B, Axial enhanced CT image shows local defect (*arrow*) of wall of right mainstem bronchus with air leaking posteriorly. Right pneumothorax and emphysema of chest wall are also confirmed.

American Journal of Roentgenology 2015.205:41-56.

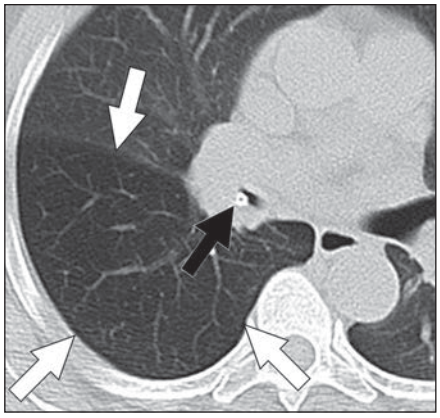

Fig. 8—63-year-old woman with history of persistent cough and foreign body aspiration. Axial CT image obtained during expiration shows tip of foreign body (*black arrow*) in bronchus intermedius and associated air trapping (*white arrows*) in right lower lobe.

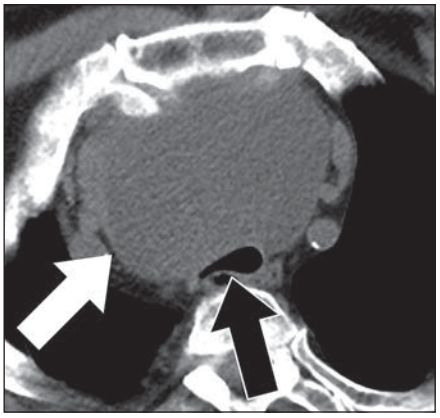

Fig. 9—62-year-old man with dyspnea and extrinsic compression of trachea. Axial CT image shows compression of trachea (*black arrow*) by soft-tissue mass (*white arrow*) within anterior mediastinum; this mass was shown to be thymic carcinoma.

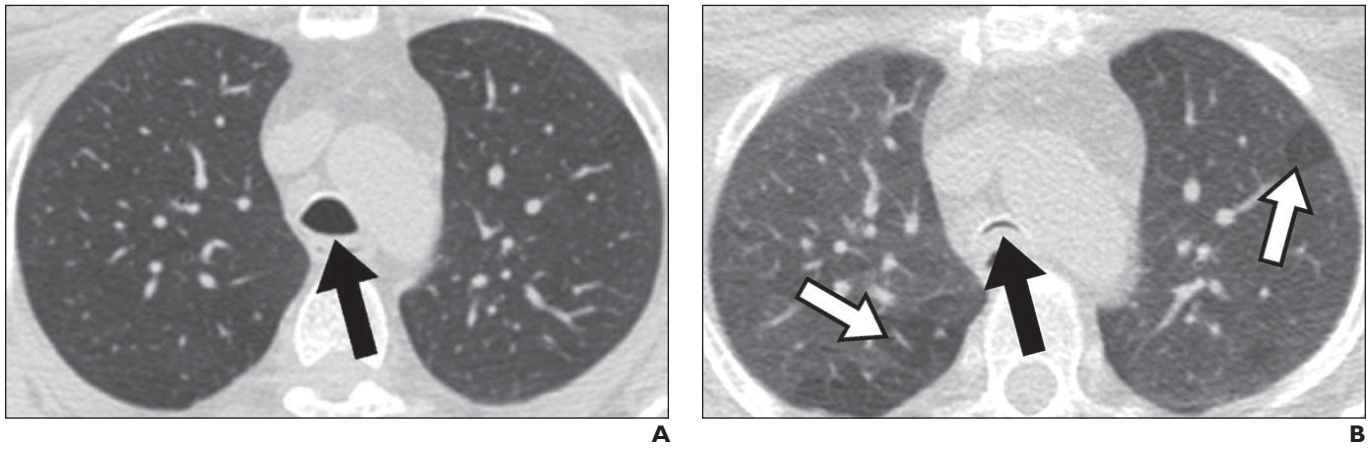

Fig. 10—54-year-old woman with tracheobronchomalacia.
A, Axial CT image obtained during inspiration shows lunate configuration of trachea (*arrow*).
B, Axial CT image obtained during expiration shows severe collapse with anterior bowing of posterior membrane (*black arrow*) ("frown" sign). Note associated air trapping (*white arrows*) in both lungs.

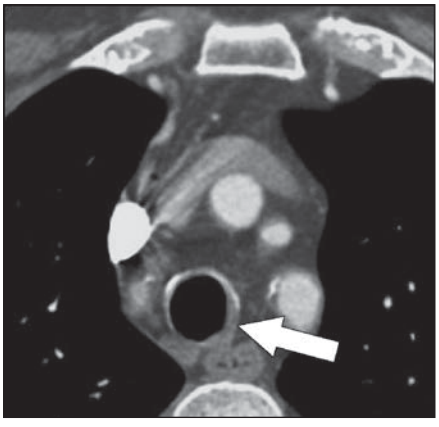

Fig. 11—71-year-old man with tracheobronchial amyloidosis. Axial enhanced CT image shows airway wall thickening (*arrow*) of left and posterior trachea.

American Journal of Roentgenology 2015.205:41-56.

Fig. 12—55-year-old woman with sarcoidosis of large airways. Axial CT image shows smooth wall thickening (*arrows*) of mainstem bronchi.

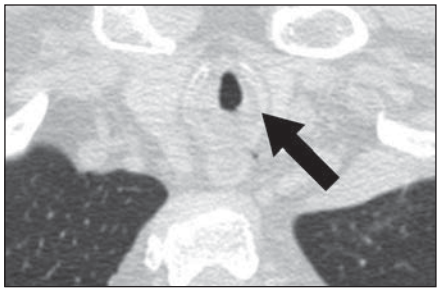

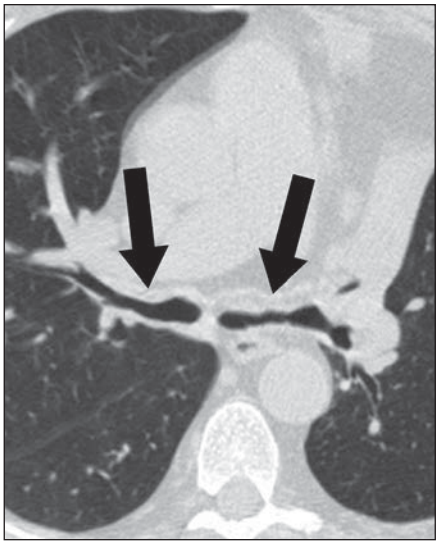

Fig. 13—73-year-old man with granulomatosis with polyangiitis.
A and **B,** Axial CT images show severe smooth wall thickening (*arrows*) of trachea (**A**) and mainstem bronchi (**B**).

Fig. 14—42-year-old man with relapsing polychondritis.
A and **B,** Axial (**A**) and sagittal reformation (**B**) CT images show diffuse coarse calcifications (*arrows*) of trachea with typical sparing of posterior membrane.

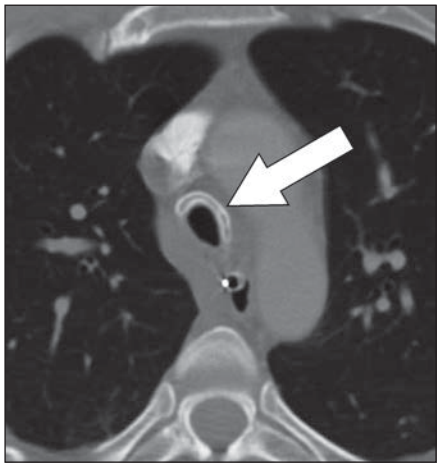

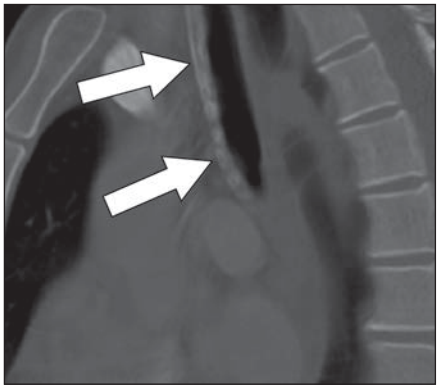

American Journal of Roentgenology 2015.205:41-56.

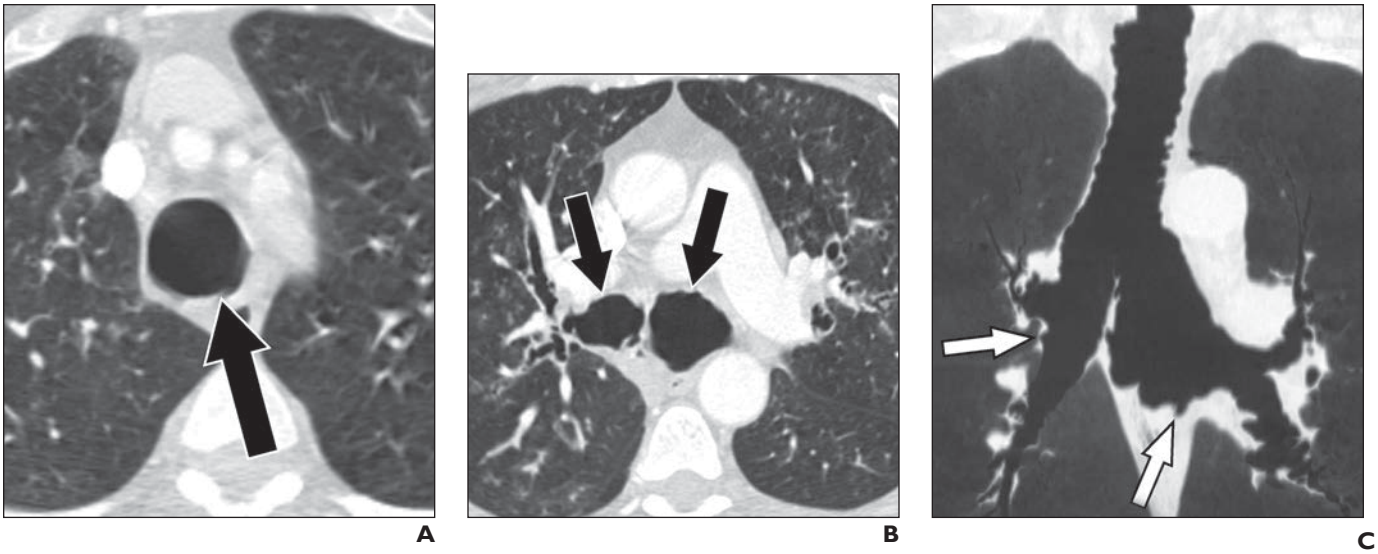

Fig. 15—58-year-old man with tracheobronchomegaly.
A and **B,** Axial CT images show dilatation (*arrows*) of trachea (**A**) and main bronchi (**B**).
C, Coronal minimum-intensity-projection CT reformation image shows dilatation of trachea and bronchi and corrugated appearance of airway wall with multiple diverticula (*arrows*).

American Journal of Roentgenology 2015.205:41-56.

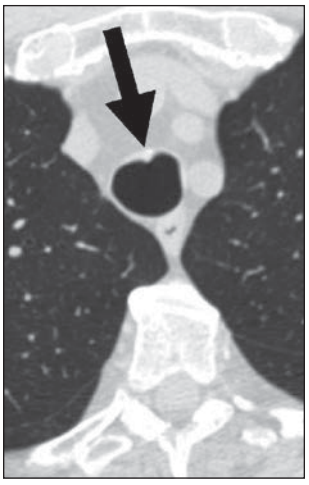

Fig. 16—80-year-old man with tracheobronchopathia osteochondroplastica. Axial CT image shows tiny nodule (*arrow*) along anterior tracheal wall with inner calcifications.

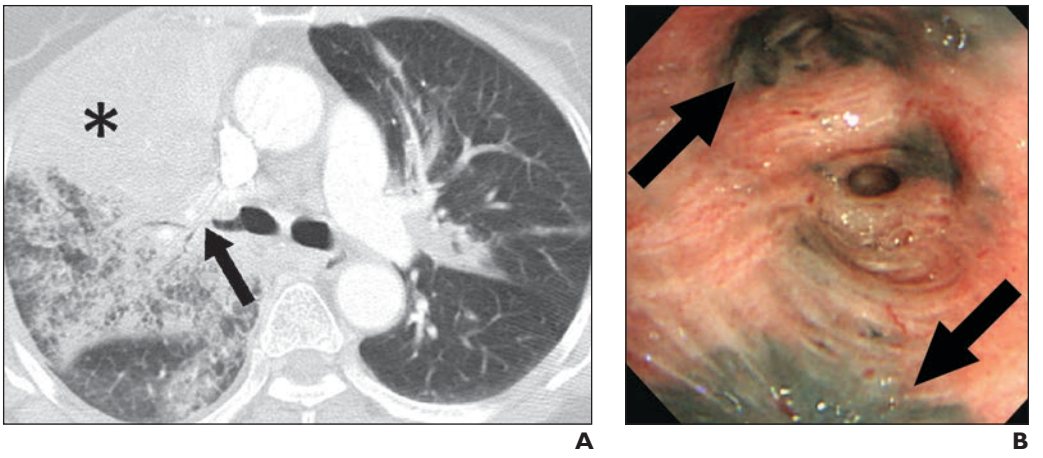

Fig. 17—70-year-old woman with anthracofibrosis and postobstructive pneumonia. (Courtesy of Lee KS, Samsung Medical Center, Seoul, Korea)
A, Axial CT image shows severe thickening of right upper lobe bronchus (*arrow*). This finding is accompanied by patchy consolidation (*asterisk*) and ground-glass opacity with septal thickening in posterior segment of right upper lobe and superior segment of right lower lobe; all of these findings are consistent with pneumonia.
B, Image of right upper lobe bronchus obtained at bronchoscopy shows dark anthracotic pigmentation (*arrows*) and narrowing of segmental bronchi.

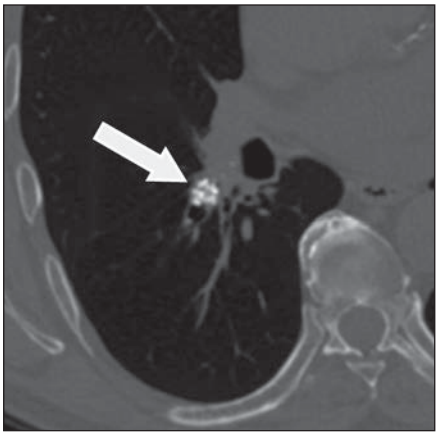

Fig. 18—67-year-old man with broncholithiasis. Axial CT image shows calcified material (*arrow*) within superior segmental bronchus of right lower lobe.

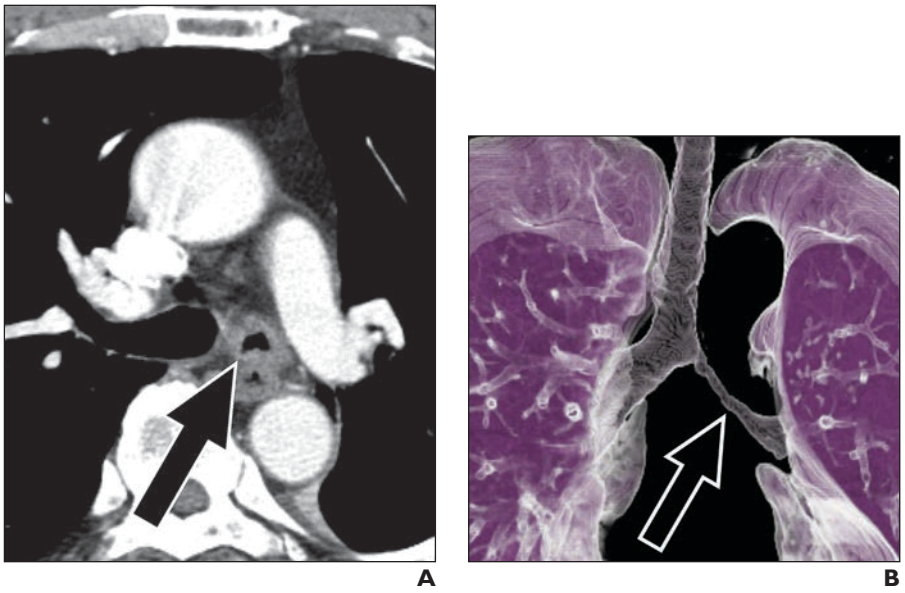

Fig. 19—57-year-old man with tuberculosis of large airways. (Courtesy of Goo JM, Seoul National University College of Medicine, Seoul, Korea)
A, Axial enhanced CT image shows irregular wall thickening (*arrow*) of left mainstem bronchus.
B, Three-dimensional reconstruction CT image shows overall extent of left mainstem bronchus stenosis (*arrow*).

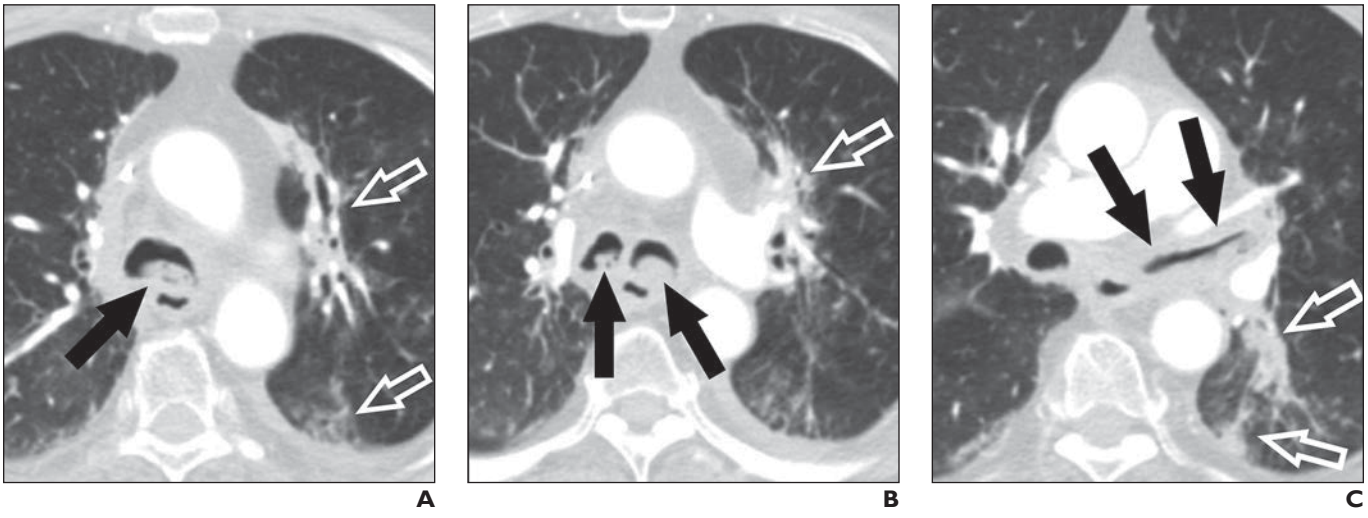

Fig. 20—65-year-old woman with aspergillosis of large airways and chronic obstructive pulmonary disease.
A and **B,** Axial enhanced CT images show soft-tissue attenuation mass (*solid arrows*) consistent with mucus and necrotic debris in dependent portion of trachea (**A**) and both main bronchi (**B**). Note small consolidations (*open arrows*) in left lung.
C, Axial enhanced CT image shows irregular wall thickening (*solid arrows*) of left mainstem bronchus. Note small consolidations (*open arrows*) in left lung.

Fig. 21—34-year-old man with papillomatosis of large airways.
A, Axial CT image shows nodular soft-tissue thickening (*arrow*) of trachea without sparing of posterior wall.
B, Axial CT image shows large cavitating nodule of soft-tissue attenuation (*black arrow*) in left lower lobe and multiple bilateral cystic lesions (*white arrows*).

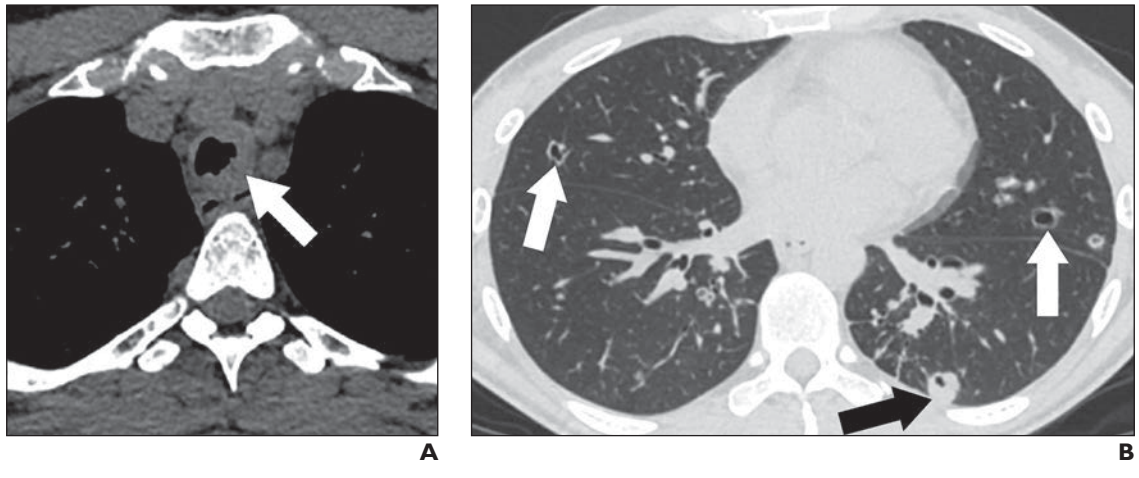

American Journal of Roentgenology 2015;205:41-56.

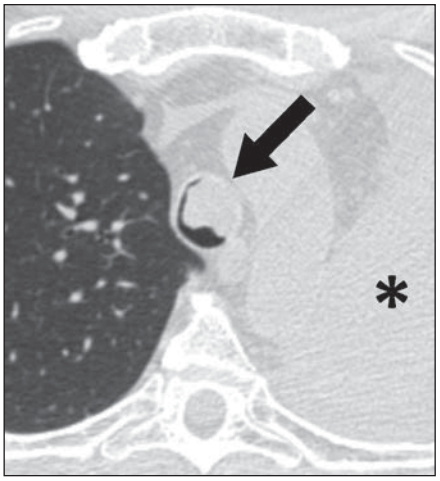

Fig. 22—61-year-old man with tracheal metastasis from rectal cancer. Axial CT image shows soft-tissue mass (*arrow*) in trachea causing reduction of tracheal lumen. Note postobstructive atelectasis of left upper lobe (*asterisk*).

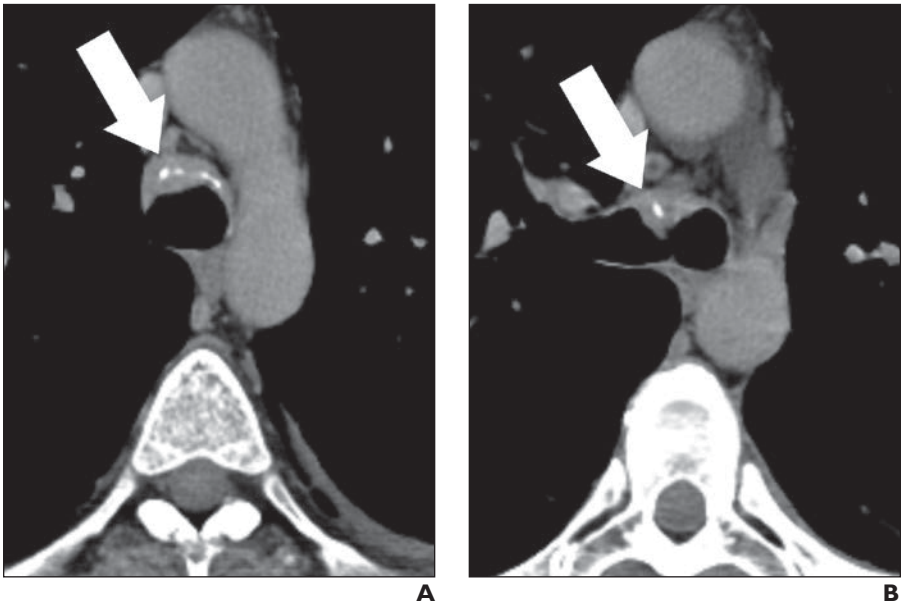

Fig. 23—58-year-old woman with adenoid cystic carcinoma.
A and **B,** Axial CT images show soft-tissue mass (*arrow*) with calcifications in anterior trachea extending toward carina (**B**).

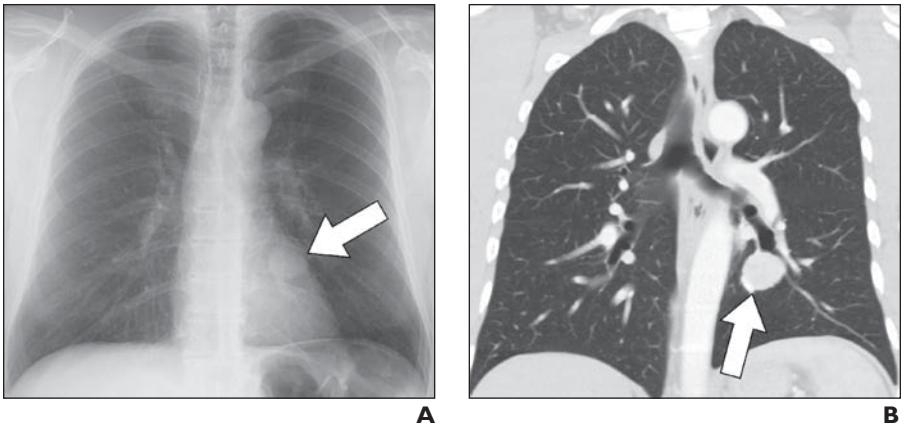

Fig. 24—44-year-old man with bronchial carcinoid tumor.
A, Posteroanterior CXR shows rounded, retrocardiac opacity (*arrow*)
B, Coronal reformation CT image shows nodule of soft-tissue density (*arrow*) in posterior basal segment of left lower lobe adjacent to segmental bronchus.

FOR YOUR INFORMATION

This article is available for CME and Self-Assessment (SA-CME) credit that satisfies Part II requirements for maintenance of certification (MOC). To access the examination for this article, follow the prompts associated with the online version of the article.

American Journal of Roentgenology 2015.205:41-56.